Acta Crystallographica Section C
Crystal Structure Communications
ISSN 0108-2701

A TiP_2O_7 superstructure

Stefan T. Norberg,* Göran Svensson and Jörgen Albertsson

Department of Inorganic Chemistry, Chalmers University of Technology, SE-412 96 Göteborg, Sweden
Correspondence e-mail: stn@inoc.chalmers.se

Received 21 September 2000
Accepted 27 November 2000

A room-temperature structural model of titanium pyrophosphate, TiP_2O_7, has been determined from synchrotron X-ray data. The structure consists of TiO_6 octahedra and PO_4 tetrahedra sharing corners in a three-dimensional network. The PO_4 tetrahedra form P_2O_7 groups connecting the TiO_6 octahedra. The $3 \times 3 \times 3$ superstructure differs substantially from the parent AB_2O_7 structure. The P—O—P bonding angles of the pyrophosphate group are between 141.21 (12) and 144.51 (13)° for those groups not located on the threefold axis. The individual TiO_6 octahedra and PO_4 tetrahedra are somewhat distorted.

Comment

The parent structure of AB_2O_7 was originally described by Levi & Peyronel (1935) with A^{IV} = Si, Ti, Zr, Sn or Hf and B^{V} = P. From powder studies, a small cubic unit cell in space group $Pa\overline{3}$ and with a = 7.80 (1) Å was found for TiP_2O_7. Further powder studies have expanded the family to include, among others, ZrV_2O_7 (Peyronel, 1942), UP_2O_7, ThP_2O_7 (Burdese & Borlera, 1963), AP_2O_7 (A = Si, Ge, Sn, Pb, Ti, Zr, Hf, Ce, U; Völlenke *et al.*, 1963), AP_2O_7 (A = Ge, Zr, U; Hagmann & Kierkegaard, 1969), HfV_2O_7 (Baran, 1976), ReP_2O_7 (Banks & Sacks, 1982), MoP_2O_7 (Kinomura *et al.*, 1985) and NbP_2O_7 (Fukuoka *et al.*, 1995). These materials have recently received renewed interest because of their small thermal expansion. Korthuis *et al.* (1995) found that ZrV_2O_7 and the mixed phase of $ZrV_{2-x}P_xO_7$, with x up to 0.3, have a negative expansion coefficient above 375 K. The materials could also be of use in high-pressure liquid chromatography as biocompatible packing materials, as suggested by Inoue & Ohtaki (1993).

Evidence of a possible $3 \times 3 \times 3$ superstructure at room temperature was first proposed by Völlenke *et al.* (1963) after careful examination of powder diffraction data for GeP_2O_7. The small AB_2O_7 parent structure had, in most cases, an unrealistically short B—O—B bridging bond distance in the B_2O_7 group, built by two connected BO_4 tetrahedra. In the smaller parent structure, all B_2O_7 groups are forced to have a 180° B—O—B bonding angle since they are located on a threefold axis. The expansions to a $3 \times 3 \times 3$ superstructure removes 96 of the 108 B_2O_7 groups in the unit cell from the threefold axis, allowing them to adopt B—O—B angles less then 180°. The ability to bend the B—O—B angle increases the bond distances for the B—O bonds connecting the BO_4 tetrahedra. For most AB_2O_7 materials, a phase transition occurs at elevated temperatures from the superstructure to the small cubic structure. ZrV_2O_7 has, for example, two phase transitions, first to an incommensurate phase at 350 K (Withers *et al.*, 1998) and then to the AB_2O_7 parent structure at 375 K (Korthuis *et al.*, 1995).

Most of the structural studies of the superstructure have been based on powder diffraction data. So far, only two single-crystal investigations of the superstructures have been published. The SiP_2O_7 superstructure suggested by Tillmanns *et al.* (1973) was limited by low resolution and therefore restricted to an isotropic model. Evans *et al.* (1998) studied the ZrV_2O_7 structure using synchrotron X-rays resulting in a model closely related to the parent AB_2O_7 structure. High-resolution neutron powder studies of ZrP_2O_7 by Khosrovani *et al.* (1996) gave P—O—P angles in the range 134–162°, which are far from the value of 180° of the parent structure. This structural model also contains a wide range of P—O bond distances, 1.44 (1)–1.66 (1) Å. Recent X-ray powder studies combined with NMR data of TiP_2O_7 by Sanz *et al.* (1997) and further NMR studies by Helluy *et al.* (2000) show a distorted structure that is less correlated to the smaller substructure. The model obtained in the powder study by Sanz *et al.* (1997) was geometrically constrained and only six isotropic displacement parameters were refined for the 50 atoms.

Small high-quality crystals of TiP_2O_7 were prepared in our search for new modifications and isomorphic materials in the KTP family of compounds (KTP = potassium titanyl phosphate, $KTiOPO_4$; Tordjman *et al.*, 1974) to improve the crystal growth and decrease the ionic conductivity. Our preparation method differs from the usual method of obtaining powder/crystals of TiP_2O_7, which is by reaction of TiO_2 and H_3PO_4 in an autoclave at temperatures around 500 K forming the hydrated phosphate α-$Ti(HPO_4)_2 \cdot H_2O$. Further calcination at temperatures around 900 K results in the formation of TiP_2O_7 (Soria *et al.*, 1993). The good quality of our crystals, prepared by the method described below, prompted us to collect TiP_2O_7 single-crystal data at the MAX II synchrotron radiation facility at Lund University, Sweden.

The TiP_2O_7 structure is built up by TiO_6 octahedra and PO_4 tetrahedra. The TiO_6 octahedra are connected by pyrophosphate groups in a three-dimensional network. Fig. 1 shows the refined TiP_2O_7 room-temperature superstructure, together with the smaller parent structure of AB_2O_7 in the (001) plane. Selected distances and angles are listed in Table 1.

The highest intensity of a superlattice reflection for ZrV_2O_7 (Evans *et al.*, 1998) was about 1% of the strongest sublattice reflection, while our data collected for TiP_2O_7 shows much stronger superlattice reflections. Table 2 gives *hkl* statistics for the TiP_2O_7 data generated by *SAINT*+ (Bruker, 1999). The mean $I/\sigma(I)$ is 114.96 for the sublattice and 41.95 for the superlattice, so a rather high proportion of the superlattice

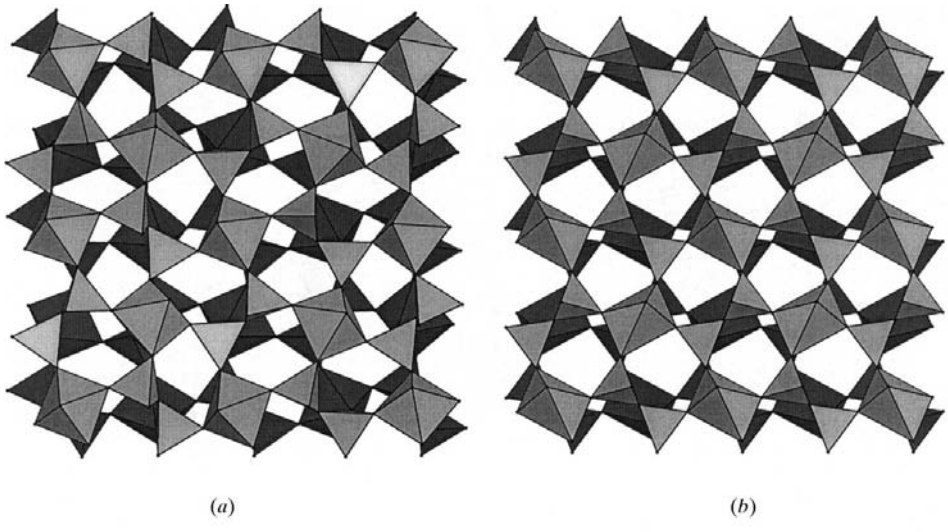

Figure 1
Two polyhedral layers showing (*a*) the TiP_2O_7 superstructure and (*b*) the substructure (Levi & Peyronel, 1935) in the (001) plane.

reflections has intensities comparable to the sublattice reflections. The highest intensity of a superlattice reflection is approximately 30% of the strongest sublattice reflection.

The TiP_2O_7 superstructure differs considerably from the parent AB_2O_7 structure, as indicated by the high intensity of the superlattice reflection ($h,k,l \neq 3n$), while the ZrV_2O_7 superstructure (Evans *et al.*, 1998) is closely related to the parent AB_2O_7 substructure. The TiO_6 octahedra and PO_4 tetrahedra in TiP_2O_7 are slightly more distorted then the ZrO_6 octahedra and VO_4 tetrahedra in ZrV_2O_7. The largest differences between the TiP_2O_7 and ZrV_2O_7 superstructures are the B—O—B bridging angles of the B_2O_7 groups located outside a threefold axis. All Ti—O bonds are in the range 1.8884 (16)–1.9453 (16) Å, with a mean bonding distance of 1.915 (14) Å. The O—Ti—O angles are between 86.75 (7) and 92.81 (8)°, while the P—O bonds in the Ti—O—P chain are in the range 1.4893 (18)–1.5069 (17) Å, with a mean bonding distance of 1.500 (5) Å. The bond angles of the PO_4 tetrahedra are between 104.16 (10) and 113.61 (10)°.

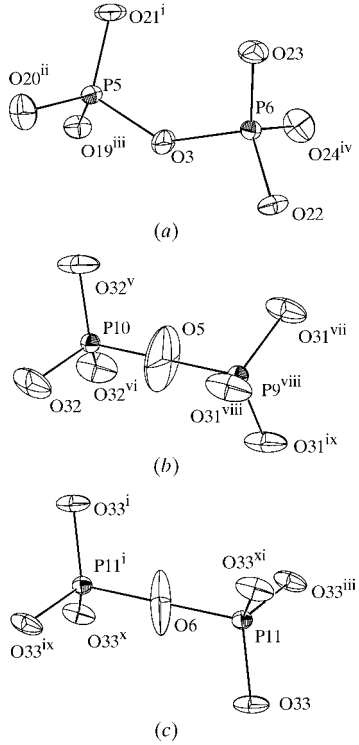

Figure 2
*ORTEP*III (Burnett & Johnson, 1996) views of different pyrophosphate groups: (*a*) shows a normal bent P_2O_7 group, while (*b*) and (*c*) show two kinds of statistical disorder on the threefold symmetry axis. Displacement ellipsoids are drawn at the 80% probability level. [Symmetry codes: (i) $1-x,-y,-z$; (ii) $1-z,1-x,-y$; (iii) $z+\frac{1}{2},-x+\frac{1}{2},-y$; (iv) $1-z,-x,-y$; (v) $1-z,x-\frac{1}{2},-y+\frac{1}{2}$; (vi) $y+\frac{1}{2},-z+\frac{1}{2},1-x$; (vii) $z+\frac{1}{2},x,-y+\frac{1}{2}$; (viii) $x+\frac{1}{2},y,-z+\frac{1}{2}$; (ix) $y+\frac{1}{2},z,-x+\frac{1}{2}$; (x) $-z+\frac{1}{2},x-\frac{1}{2},y$; (xi) $-y+\frac{1}{2},-z,x-\frac{1}{2}$.]

There are six independent P_2O_7 groups in the unit cell, two of them are constrained to a 180° P—O—P bridging angle, while the other four have P—O—P angles of 141.21 (12)–144.51 (13)° between the PO_4 tetrahedra. This is in good agreement with the combined X-ray powder diffraction/NMR study on TiP_2O_7 by Sanz *et al.* (1997), who reported bridging P—O—P angles in the range 139–145°. The mean P—O bond in the P—O—P bridge for the four unconstrained pyrophosphate groups is 1.575 (5) Å compared with 1.536 (4) Å for the constrained ones. The O5 and O6 atoms bridging PO_4 tetrahedra in the two pyrophosphate groups located at a threefold axis show enlarged displacement parameters compared with all other O atoms, as can be seen in Fig. 2, indicating the structural disorder previously suggested by Sanz *et al.* (1997). The P9—O5—P10 pyrophosphate group seems to have an unlimited number of possible bond configurations, as shown by the shape of the displacement parameter, while P11—O6—P11 has two possible bond configurations, as can be seen in the displacement ellipsoid plot in Fig. 2. The ZrV_2O_7 (Evans *et al.*, 1998) superstructure does not show any enlarged displacement parameters for the O atoms at a threefold axis and has V—O—V angles in the range 159.3 (2)–167.6 (2)°.

Experimental

The crystals were obtained by spontaneous crystallization from a flux, in a platinum crucible, containing $Zn_3(PO_4)_2$, P_2O_5, ZnO and TiO_2 carefully mixed together in the molar ratio 1.00:1.55:0.55:1.10. The flux were first dehydrated at 523 K for 15 h and then heated to 1373 K, after which the temperature was decreased to 1073 K at a rate of 2.3 K h^{-1}. The flux was dissolved in 6 *M* HCl and the result was a crystalline powder with a weak orange colour. Energy dispersive X-ray (EDX) analysis (Electro-scan S4–8DV equipped with a Link eX1 EDX system) indicates no zinc on any of the small well developed crystal faces.

Crystal data

TiP_2O_7
M_r = 221.82
Cubic, $Pa\bar{3}$
a = 23.5340 (5) Å
V = 13034.3 (5) Å^3
Z = 108
D_x = 3.052 Mg m^{-3}
Synchrotron X-ray vertical wiggler radiation
λ = 0.8522 (5) Å
Cell parameters from 7382 reflections
θ = 3.60–43.45°
μ = 3.74 mm^{-1}
T = 293 (1) K
Rectangular, colourless
0.06 × 0.02 × 0.02 mm

Data collection

Bruker SMART area 1000 CCD diffractometer
Area-detector scans
Absorption correction: multi-scan (*SADABS*; Bruker, 1998)
T_{min} = 0.619, T_{max} = 0.923
82 262 measured reflections
8970 independent reflections
8363 reflections with $F > 4\sigma(F)$
R_{int} = 0.099
θ_{max} = 43.51°
$h = -30 \rightarrow 26$
$k = -36 \rightarrow 35$
$l = -34 \rightarrow 20$
Intensity decay: adjusted for decay by flux statistics for each frame

Refinement

Refinement on F
R = 0.046
wR = 0.059
S = 2.872
8563 reflections
408 parameters
$w = 1/\sigma^2(F)$
$(\Delta/\sigma)_{max}$ = 0.002
$\Delta\rho_{max}$ = 1.14 e Å^{-3}
$\Delta\rho_{min}$ = −1.29 e Å^{-3}
Extinction correction: Gaussian (Zachariasen, 1967)
Extinction coefficient: 2303 (43)

Table 1
Selected geometric parameters (Å, °).

P1—O1	1.5770 (19)	P7—O4	1.5662 (19)
P2—O1	1.578 (2)	P8—O4	1.5815 (18)
P3—O2	1.5805 (18)	P9—O5^{i}	1.541 (2)
P4—O2	1.5770 (19)	P10—O5	1.536 (2)
P5—O3	1.5726 (17)	P11—O6	1.5332 (5)
P6—O3	1.5707 (18)		
P1—O1—P2	144.51 (13)	P5—O3—P6	141.21 (12)
P3—O2—P4	143.04 (12)	P7—O4—P8	143.41 (12)

Symmetry codes: (i) $x-\frac{1}{2}, y, \frac{1}{2}-z$; (ii) $\frac{1}{2}+x, y, \frac{1}{2}-z$; (iii) $1-x, -y, -z$.

The X-ray beam at the MAX II beamline 711 (Cerenius *et al.*, 2000) was focused vertically by a bendable quartz mirror coated with platinum and horizontally by an asymmetrically cut Si(111) monochromator (an asymmetric angle of 7° was used). A 100 µm collimator with an inherent ionization chamber/counting device and the program *SAINT*+ (Bruker, 1999) were used to adjust for the intensity changes during the data collection. The different series of frames were later normalized with *SADABS* (in *SAINT*+). The X-ray wavelength was calibrated against Si powder. A total of eight series of frames were collected over 11 h, with a nominal measuring time of 2 s per frame. The systematic absences ($0kl$, $k = 2n+1$, and $00l$, $l = 2n+1$) suggested the space group $Pa\bar{3}$ (# 205). 200 weak reflections with $F < 4\sigma(F)$, that had no effect on the final structural model except for improving the s.u.'s of some atoms, were added during the final least-squares refinement. Anomalous scattering factors for neutral atoms for the appropriate wavelength were taken from Sasaki (1989). The linear absorption coefficient μ was calculated using mass attenuation coefficients for neutral atoms at the wavelength 0.8522 Å (Sasaki, 1990). About 0.5% of the reflections were affected by extinction (Zachariasen, 1967), with a maximum correction of $y = 0.76$ for the 006 reflection (the observed structure factor is $F_{obs} = yF_{kin}$, where F_{kin} is the kinematic value of the structure factor).

Data collection: *SMART–NT* (Bruker, 1998); cell refinement: *SAINT*+ (Bruker, 1999); data reduction: *SAINT*+ and *Xtal*3.7 (Hall *et al.*, 2000); program(s) used to refine structure: *SHELXL*97 (Sheldrick, 1997) and *Xtal*3.7; molecular graphics: *ORTEP*III (Burnett & Johnson, 1996).

Table 2
Intensity statistics for all measured reflections.

$I/\sigma(I)$ interval	Number of superlattice ($h,k,l \neq 3n$) reflections	Number of sublattice ($h,k,l = 3n$) reflections
0.00–1.00	7467	231
1.00–2.00	4572	58
2.00–4.00	8257	89
4.00–8.00	11641	135
8.00–16.00	17509	330
16.00–32.00	18779	525
32.00–64.00	9022	591
64.00–128.00	1957	652
128.00–256.00	28	419

The authors would like to thank Yngve Cerenius at beamline 711 (MAX II) for assistance during the data collection. This work was supported by the Chalmers Foundation and the Swedish Technical Research Council (TFR).

Supplementary data for this paper are available from the IUCr electronic archives (Reference: BR1307). Services for accessing these data are described at the back of the journal.

References

Banks, E. & Sacks, R. (1982). *Mater. Res. Bull.* **17**, 1053–1055.
Baran, E. J. (1976). *J. Less Common Met.* **46**, 343–345.
Bruker (1998). *SMART–NT*. Version 5.050. Bruker AXS Inc., Madison, Wisconsin, USA.
Bruker (1999). *SAINT*+. Version 6.01 (includes *XPREP* and *SADABS*). Bruker AXS Inc., Madison, Wisconsin, USA.
Burdese, A. & Borlera, M. L. (1963). *Ann. Chim. Rome*, **50**, 1570–1583.
Burnett, M. N. & Johnson, C. K. (1996). *ORTEP*III. Report ORNL-6895. Oak Ridge National Laboratory, Tennessee, USA.
Cerenius, Y., Ståhl, K., Svensson, L. A., Ursby, T., Oskarsson, Å., Albertsson, J. & Liljas, A. (2000). *J. Synchrotron Rad.* **7**, 203–208.
Evans, J. S. O., Hanson, J. C. & Sleight, A. W. (1998). *Acta Cryst.* B**54**, 705–713.
Fukuoka, H., Imota, H. & Saito, T. (1995). *J. Solid State Chem.* **119**, 98–106.
Hagmann, L. O. & Kierkegaard, P. (1969). *Acta Chem. Scand.* **23**, 327–328.
Hall, S. R., du Boulay, D. J. & Olthof-Hazekamp, R. (2000). Editors. *Xtal*3.7 *System*. University of Western Australia, Australia.
Helluy, X., Marichal, C. & Sebald, A. (2000). *J. Phys. Chem. B*, **104**, 2836–2845.
Inoue, S. & Ohtaki, N. (1993). *J. Chromatogr.* **645**, 57–65.
Khosrovani, N., Korthuis, V., Sleight, A. W. & Vogt, T. (1996). *Inorg. Chem.* **35**, 485–489.
Kinomura, N., Hirose, M., Kumada, N. & Muto, F. (1985). *Mater. Res. Bull.* **20**, 379–382.
Korthuis, V., Khosrovani, N., Sleight, A. W., Roberts, N., Dupree, R. & Warren, W. W. (1995). *Chem. Mater.* **7**, 412–417.
Levi, G. R. & Peyronel, G. (1935). *Z. Kristallogr.* **92**, 190–209.
Peyronel, G. (1942). *Gazz. Chim. Ital.* **72**, 83–88.
Sanz, J., Iglesias, J. E., Soria, J., Losilla, E. R., Aranda, M. A. G. & Bruque, S. (1997). *Chem. Mater.* **9**, 996–1003.
Sasaki, S. (1989). *Numerical Tables of Anomalous Scattering Factors, Calculated by the Cromer and Mann's Method*. KEK Report 88–14, pp. 1–136.
Sasaki, S. (1990). *X-ray Absorption Coefficients for the Elements (Li to Bi, U)*. KEK Report 90–16, pp. 1–143.
Sheldrick, G. M. (1997). *SHELXL*97. University of Göttingen, Germany.
Soria, J., Iglesias, J. E. & Sanz, J. (1993). *J. Chem. Soc. Faraday Trans.* **89**, 2515–2518.
Tillmanns, E., Gebert, W. & Baur, W. H. (1973). *J. Solid State Chem.* **7**, 69–84.
Tordjman, I., Masse, R. & Guitel, J. C. (1974). *Z. Kristallogr.* **139**, 103–115.
Völlenke, H., Wittman, A. & Nowotny, H. (1963). *Monatsh. Chem.* **94**, 956–963.
Withers, R. L., Evans, J. S. O., Hansson, J. & Sleight, A. W. (1998). *J. Solid State Chem.* **137**, 161–167.
Zachariasen, W. H. (1967). *Acta Cryst.* **23**, 558–564.